CONCLUSION

Conventional methods of flood frequency analysis often are not suitable for watersheds in which conditions are changing with time. For such cases, a versatile alternative is time-series analysis, which considers the magnitude, the frequency, and the sequential order of the flood data. The time-series approach is formulated to reflect the factors and circumstances that significantly influence peak flows. Consequently, resulting flood estimates are representative of prevailing watershed conditions.

REFERENCES

1. B.M. Reich. Magnitude and Frequency of Floods. CRC Critical Reviews in Environmental Control, Vol. 6, No. 4, 1976, pp. 297-348.
2. A Uniform Technique for Determining Flood Flow Frequencies. Water Resources Council, Bull. 15, 1967.
3. Guidelines for Determining Flood Flow Frequency. Water Resources Council, Bull. 17, 1976.
4. Guidelines for Determining Flood Flow Frequency, rev. ed. Water Resources Council, Bull. 17A, 1977.
5. A.F. Huggins and M.R. Griek. Hydrologic Report of Colorado River-Glenwood Canyon. Barton, Stoddard, Milhollin and Higgens, Inc., Denver, CO, 1969, 34 pp.
6. S.G. Buchberger. Hydrologic Analysis of the Colorado River at Glenwood Canyon, Colorado. Colorado Department of Highways, Denver, Open-File Rept., 1979, 57 pp.
7. V. Yevjevich. Stochastic Processes in Hydrology. Water Resources Publications, Fort Collins, CO, 1972a, 276 pp.
8. C.T. Haan. Statistical Methods in Hydrology. Iowa State Univ. Press, Ames, 1977, 378 pp.
9. V. Yevjevich and R.I. Jeng. Properties of Non-Homogeneous Hydrologic Series. Colorado State Univ., Fort Collins, Hydrology Paper 32, 1969, 33 pp.
10. N.C. Matalas. Time Series Analysis. Water Resources Research, Vol. 3, No. 3, 1967, pp. 817-828.
11. G.W. Kite. Frequency and Risk Analyses in Hydrology. Water Resources Publications, Fort Collins, CO, 1977, 224 pp.
12. U.S. Bureau of Reclamation. Annual Operating Plan of Western Division, 1978-1979. U.S. Department of the Interior, 1978, 41 pp.
13. L.R. Beard and A.J. Fredrich. Hydrologic Frequency Analysis. Hydrologic Engineering Methods for Water Resources Development, Vol. 3, 1975.
14. V. Yevjevich. Probability and Statistics in Hydrology. Water Resources Publications, Fort Collins, CO, 1972b, 302 pp.
15. R.D. Markovic. Probability Functions of Best Fit to Distributions of Annual Precipitation and Runoff. Colorado State Univ., Fort Collins, Hydrology Paper 8, 1965, 33 pp.

Publication of this paper sponsored by Committee on Hydrology, Hydraulics, and Water Quality.

Dynamics Approach for Monitoring Bridge Deterioration

H.J. SALANE, J.W. BALDWIN, JR., AND R.C. DUFFIELD

In conjunction with a fatigue test of a full-scale in situ three-span highway bridge, an investigation was undertaken to evaluate the use of changes in dynamic properties of the bridge as a possible means of detecting structural deterioration due to fatigue cracks in the girders. Cyclic-loading tests (transient and steady-state) were conducted to determine the changes in dynamic properties. The loading was imposed by a moving-mass, closed-loop electrohydraulic actuator system. Several different dynamic tests were employed in the investigation to determine the modal viscous damping ratios, stiffness, and mechanical impedance of the bridge at selected intervals during the fatigue loading. Acoustic emission sensors were also used to monitor the growth of fatigue cracks in the girders. The results show that changes in the bridge stiffness and vibration signatures in the form of mechanical-impedance plots are indicators of structural deterioration caused by fatigue. Stiffness coefficients were calculated from the experimental mode shapes on the basis of a multi-degree-of-freedom system that uses modified coupling. The average reduction in stiffness was approximately 20 percent. This reduction was attributed to the combined deterioration of the bridge deck and steel girders. Mechanical-impedance plots were made from frequency-sweep tests, which included five resonant modes. Early changes in the mechanical-impedance plots were related to the deterioration of the bridge deck. Subsequent changes in these plots correlated with the fatigue cracking in the steel girders. An evaluation of the acoustic emission data showed that the sensors were able to detect the rapid critical crack growth in one girder.

At this time there is a substantial amount of research under way on the techniques used for monitoring structural deterioration. The types of techniques may be broadly classified under the following categories--nondestructive-testing methods and vibration-response methods. Much of the recent development in vibration-analysis techniques for monitoring structural integrity (1-4) stems from the needs of the offshore industry.

In general, nondestructive-testing procedures can be time-consuming and costly. This becomes evident when the structures are large, such as multispan bridges and offshore platforms. Nonetheless, the nondestructive tests that involve ultrasonic examinations and visual inspection are two of the most effective means of locating deterioration in a structure. As a consequence of the cost and time involved to accomplish nondestructive tests, alternative methods that will reduce the frequency of these tests are desirable.

Typically, a vibration-response method employs accelerometers to measure the response of the structure from either environmental forces or applied excitation forces. The data are analyzed to establish prescribed dynamic system parameters. Any significant changes in subsequent evaluations of these parameters are interpreted as fatigue damage in structural members or foundation settlement. In this approach to monitoring, vibration-response data provide a surveillance of the structure on a broad basis.

Many of today's highway bridges have a multitude of welded connections and details. These weldments

contain microscopic flaws from which cracks may initiate and propagate under service loading. Visual and ultrasonic examinations have shown that welded steel-girder bridges are prone to fatigue cracking. When a three-span continuous composite-girder highway bridge in Butler County, Missouri, was scheduled for removal, an in situ fatigue test to destruction of the full-scale structure was proposed. The aim of the study was to document the fatigue behavior of the bridge and to relate this behavior to the design specifications for highway bridges of the American Association of State Highway Officials (AASHO).

Another objective of the study was to evaluate several vibration-response methods for monitoring structural deterioration. This paper describes the evaluation of the following vibration-response methods: (a) transient, frequency-response, and sweep tests for the properties of an equivalent 1-degree-of-freedom (df) model, (b) steady-state normal mode tests for the properties of a multi-df model, and (c) acoustic emission measurements of fatigue-crack growth. Previous publications (5,6) contain a description of the instrumentation and data evaluation. For completeness, some material from the earlier publications is included in this paper.

DESCRIPTION OF TESTS

Four sets of dynamic tests were conducted on the in situ bridge. The first set was performed prior to initiating the fatigue tests. After 95 000 and 215 000 fatigue cycles, the fatigue test was interrupted and the second and third sets of dynamic tests were conducted. The fourth set of tests was performed at 377 000 fatigue cycles after the south interior girder had fractured at midspan.

In addition to the dynamic tests, 14 sets of acoustic-emission measurements at 8 locations on the girders were recorded without interrupting the fatigue test.

TEST BRIDGE

The two-lane, three-span [22, 28, and 22 m (72, 93, and 72 ft)] continuous composite-girder bridge was designed in 1962 in accordance with 1961 AASHO specifications for one-lane H15-44 loading. Principal features of the bridge are shown in Figure 1. Four flange girders of ASTM A-36 steel 76 cm (30 in) wide cover-plated over the main piers supported a 15-cm (6-in) concrete slab designed for composite action in the positive-movement regions. The slab concrete had a 28-day compressive strength of 36.3 MPa (5.27 ksi). Shear connectors were C4x5.4 channels 159 mm (6.25 in) long fillet-welded to the top flanges of the girders except in the cover-plated regions over the piers. The abutments and piers were supported by precast concrete piles driven to a minimum capacity of 0.285 MN (32 tons) in sand.

VIBRATION GENERATOR

Excitation force for all dynamic tests was supplied by a closed-loop electrohydraulic actuator system. Steel plates that weighed 4973 N (1115 lb) were attached to the top of the piston rod of the actuator. The actuator was mounted in the vertical position at designated stations on the upper side of the bridge deck. Locations of the actuator for the dynamic tests were at stations (Figure 2) 17, 16, 5, and 4 for the first bending mode, first torsional mode, second bending mode, and the sweep tests, respectively. During all the tests the maximum acceleration of the bridge deck was less than 0.7 g. The basic closed-loop system provided stroke and sinusoidal frequency control of the motion of the actuator. The excitation force was prescribed by controlling the relative acceleration of the moving weight with respect to the base of the actuator in a secondary control loop.

INSTRUMENTATION

Piezoresistive accelerometers that had a rating of 25 g were used to establish the relative acceleration of the moving weight and thereby control the excitation force that was applied during the dynamic tests. Servo accelerometers based on the Q-flex design with a range ±15 g were used to measure the vertical accelerations of the bridge at prescribed locations, which had been designated as stations, on the underside of the bridge. These stations are shown in Figure 2. Signals from the accelerometers were filtered with low-pass electronic filters set at 10 Hz.

DATA ACQUISITION

The primary data-acquisition system for the dynamic tests was an analog-to-digital converter and a tape transport. During the tests, the data channels were automatically scanned, sampled, and digitized at a prescribed rate of 70 or 100 times per second. The tape-transport unit wrote 12-bit data words into a nine-track magnetic tape at a density of 800 bits/in. For a backup data acquisition system, a light-beam multichannel strip-chart recorder was used to obtain an analog record of the test data.

TEST PROCEDURES

In the bridge test, each set of dynamic tests was made up of the following vibration-response techniques: (a) transient test, (b) frequency-response test, (c) sweep test, and (d) steady-state normal mode test.

For the transient, frequency-response, and normal mode tests, each test was conducted at three prescribed resonant frequencies of the bridge. The frequencies were associated with the following experimentally determined vibrational modes: (a) first (lowest) bending, (b) first (lowest) torsional, and (c) second bending. These modes were designated B1J, T1J, and B2J, respectively, in which J refers to the test set numbers, i.e., J = 1,2,3,4.

Transient Test

In the transient tests the bridge was excited to a steady-state condition at the frequency that corresponded to the prescribed mode. Then the hydraulics to the actuator was turned off. This produced a transient decaying response motion in the bridge. Thirty seconds of acceleration-response data were recorded at stations 17, 16, and 5 for modes B1, T1, and B2, respectively. Data from these tests were used to establish the damping ratio ζ from the log decrement curves.

Frequency-Response Test

The frequency-response tests were conducted to establish the frequency-response curves for each of the three vibrational modes. Response data for these curves were recorded at 30 increments of frequency. By this procedure a frequency range of ±0.2 Hz about the resonant frequency was covered. The bridge was allowed to reach a steady-state response condition at each increment of frequency prior to recording the accelerations at stations 5, 17, and

Figure 1. Test bridge.

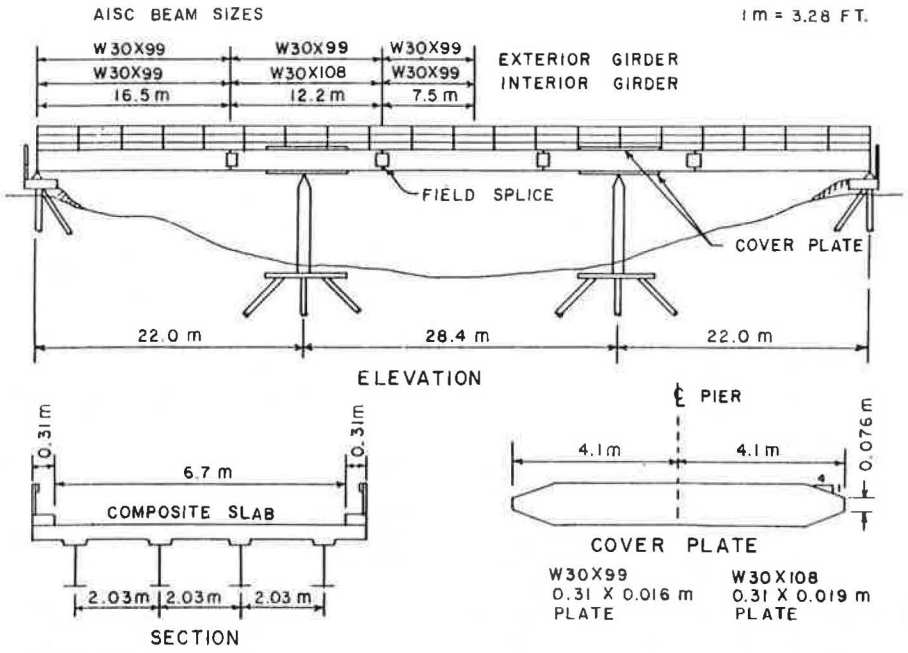

Figure 2. Accelerometer stations on bridge.

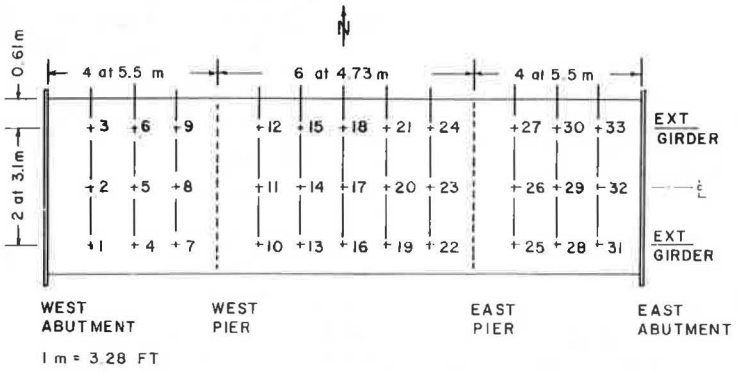

29 for the first bending mode; stations 4, 16, and 28 for the first torsional mode; and stations 5, 14, and 29 for the second bending mode. A constant excitation force was maintained during all tests. Response data were recorded for each frequency range beginning at the low end of the frequency range and increasing the frequency for each successive increment. Subsequently, the test was repeated beginning at the high end of the frequency range and decreasing the frequency for each successive increment. Data from these tests were used to calculate the damping ratio ζ by the half-power-bandwidth procedure.

Sweep Test

Sweep tests were performed to establish vibration signatures for the bridge in the form of mechanical impedance graphs. The frequency range of the sweep covered the lowest five experimentally determined resonant frequencies. A linear sweep rate of 0.02 Hz/s for a sine-wave excitation was used, and the test was initiated at the low end of the frequency spectrum. Continuous-response acceleration data were recorded at stations 4, 9, 15, and 30 during a 3-min time interval.

Normal Mode Test

Steady-state normal mode tests were conducted at each of the three resonant frequencies. One servo accelerometer was used as a fixed reference while the other accelerometer was moved from station to station to capture the response data. A minimum of 1024 data points was recorded at each station to establish the amplitude and phase of the steady-state motion with respect to the reference station. For the purpose of these tests the acceleration response was measured at 22 stations on the underside of the bridge. All 11 stations that were along the south exterior girder and all 11 stations along the north exterior girder were used. Stations along the centerline of the bridge were not used. From the test data, damping and stiffness coefficients of the bridge were calculated.

Acoustic-Emission Test

Eight acoustic-emission sensors were also used to monitor the growth of fatigue cracks in the steel girders during the fatigue test. State-of-the-art acoustic-emission equipment, which was readily available, was employed for this purpose. Each sensor was clamped to the bottom flange of a steel girder within 15 cm (6 in) of the end of a cover

plate. Sensors 1, 2, 3, and 4 were located in the west end span on the south exterior, south interior, north interior, and north exterior girders, respectively. Sensors 5, 6, 7, and 8 were located in the east end span on the south exterior, south interior, north interior, and north exterior girders, respectively. In operation, the sensors were individually monitored by manual switching. Fourteen sets of data were recorded during the course of the fatigue test. An amplitude count of acoustic emission per second over a 150-s interval was plotted versus time on an XY-recorder. In a time interval of 150 s, the bridge underwent approximately 300 cycles of vibration. The analog acoustic emission signals were amplified with gains that ranged from 72 to 82 dB. The resonant frequency of a sensor was 230 kHz, and an electronic filter was set to bandpass frequencies in the range of 100-400 kHz.

Acoustic-emission monitoring was initiated when the bridge had accumulated 56 000 fatigue cycles. At the outset of monitoring there appeared to be a repetitive noise in the emission signal when the center span of the bridge was in its most upward position. This noise was attributed to the vibration generator. Consequently, the acoustic-emission count was inhibited over that part of the vibration cycle. After 315 000 fatigue cycles, the inhibit circuitry was disconnected because of a malfunction in the electronics.

DISCUSSION OF RESULTS

The results from an evaluation of the data are presented to provide comparison of the various vibration-response methods. Lindner (5) and Brady (6) have provided a mathematical development of the equations used in the data evaluation.

Transient Test

On the basis that the bridge was excited in a single mode, the logarithmic-decrement method was applied to the decaying response data to determine the damping ratio ζ as a function of the number of free vibration cycles. Figure 3 illustrates the variation in ζ during a 35-cycle interval for test 2.

An alternate approach was adopted to evaluate the damping in tests 3 and 4 due to the multifrequency components that were observed in the transient-response data. Damping ratios were obtained by transforming the data from the time domain to the frequency domain. This procedure effectively separates the multifrequency components and is based on the properties of the discrete Fourier transform. Damping ratios for three modes in the four tests are listed in Table 1. The damping values for all three spans in each mode are consistent. It is also apparent that the damping increased from test 1 to test 2 and then decreased in tests 3 and 4.

Frequency-Response Tests

Analog data from the frequency-response tests were filtered by means of a 10-Hz low-pass filter prior to the analog-to-digital conversion. However, because of other frequency components in the response, the digital data were further filtered by a fast-Fourier-transform technique in order to isolate the amplitude of the response at each specific frequency increment. Figure 4 illustrates response graphs for the first bending mode, test 3. On the basis of the half-power bandwidth, the values of ζ that were calculated are listed in Table 2. Although there is a variation in the damping values between each span and for each set of tests, the range of ζ is consistently between 1 and 3 percent. The damping ratios reported in Table 2 are average values from the data obtained when the test was initiated at the low end of the frequency range and then subsequently repeated beginning at the high end of the frequency range.

Sweep Test

Mechanical impedance is defined as the ratio of the excitation force to steady-state velocity for sinusoidal motion. The resulting ratio is a complex quantity that may be represented by a magnitude and phase angle. If the force is applied at one location on the structure and the response velocity is determined at another location, the ratio is referred to as transfer impedance. However, if the force and velocity are located at the same place in the structure, the ratio is referred to as driving-point impedance. Minimum points on the mechanical impedance graph are associated with a resonant frequency of the structure. At resonance the phase angle between the excitation force and the response velocity is zero (or 180 degrees). Maximum ordinates on the impedance graph are called antiresonant points.

The intent in the sweep test was to maintain a constant force level throughout the frequency range. However, the amplitude controller was not able to maintain this condition at the high end of the frequency range. For a linear elastic system the mechanical impedance is independent of the excitation force. The frequency-response test data did not exhibit the jump phenomenon in the vicinity of the resonant response, which would have been an indication of nonlinear behavior. Thus, the assumption that the bridge was a linear elastic system was reasonably valid.

Figures 5 and 6 illustrate the variation in driving-point and transfer impedances for tests 3 and 4. A notable change in the impedance occurred between tests 1 and 2. The resonant frequencies decreased and the magnitudes of the impedance increased. This increase implies that the equivalent damping increased. The reduction in resonant frequencies was associated with the deterioration of the bridge deck.

The change in impedance between tests 2 and 3 was minimal. However, the lower resonant frequencies increased slightly, which was unexpected. The largest variation in impedance between tests 3 and 4 occurred at the higher resonant frequencies. Test 4 was conducted after the fracture had occurred in the south interior girder at the midpoint in the center span.

Normal Mode Test

Four sets of normal mode tests at three resonant frequencies were performed to evaluate the stiffness and damping properties of the bridge as the fatigue test progressed. A spectral analysis of the data revealed a harmonic component in the first-bending-mode data from tests 3 and 4. Figure 7 illustrates that the amplitude of the harmonic increased between tests 3 and 4. The harmonic in test 4 was anticipated because of the fracture in the girder. In the first bending mode the fracture was located at a point of maximum deflection, whereas in the second bending mode the fracture was located at a point of zero deflection (i.e., a vibrational node). However, in the torsional mode, the fracture was located at a point of one-half the maximum deflection, but the spectrum of the torsional data did not reveal any harmonics.

In order to establish the amplitudes for the mode shapes, all data were digitally filtered by an ex-

Figure 3. Damping ratio from logarithmic-decrement method.

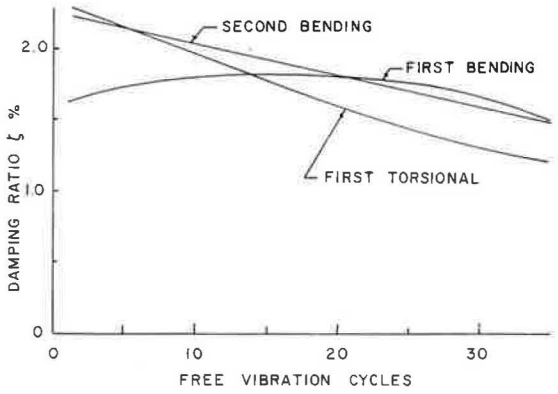

Table 1. Damping ratios and frequencies determined by Fourier-transform decay method.

Test No.	Frequency (Hz)	Damping Ratio (% critical) by Span		
		East	Center	West
First Bending				
1	2.92 (2.90)[a]	1.0	1.1	1.0
2	2.66 (2.73)	2.6	2.5	2.5
3	2.67	2.2	2.2	2.1
4	2.49	2.9	--	2.5
First Torsion				
1	3.62 (3.60)	1.7	1.6	1.7
2	3.34 (3.42)	3.3	3.3	--
3	3.11	3.2	3.1	3.0
4	3.19	2.6	2.7	2.7
Second Bending				
1	4.59 (4.57)	1.1	--	1.3
2	4.23 (4.28)	2.8	--	2.7
3	4.29	2.1	2.1	2.2
4	4.14	2.2	2.1	2.1

[a]Numbers in parentheses indicate damped natural frequency determined from the time-transient response signal.

tended cosine-bell window and analyzed by a fast-Fourier-transform technique. The spectral amplitudes were also normalized with respect to the spectral amplitudes at the reference station.

Since the bridge was assumed to have 22 df for vertical motion and three vibrational modes were measured, 66 equations were established to determine the stiffness and damping properties for the analytical model from the normal mode equations of motion. Because of the limited number of simultaneous equations, the coupling between the 22 nodes in the analytical model was arbitrarily assumed so that the bandwidth of the stiffness and damping matrices was 5. For the assumed coupling and utilizing symmetry, there are 63 unknown coefficients in the 22-df stiffness and damping matrices. The diagonal coefficients were assumed to be most significant and were used to monitor the change in properties during the fatigue test.

Figure 8 illustrates the relative changes in the stiffness coefficients between tests 1 and 3 and tests 1 and 4 for the stations on the north and south sides of the bridge. For the most part the reduction in stiffness coefficients was greater between tests 1 and 4 than between tests 1 and 3. The reduction in stiffness between tests 1 and 4 was also greater for the south side of the bridge, which correlates with the fracture in the south interior girder. The reason for the large variation in the coefficients for the east end of the bridge is not known.

Figure 4. Frequency response, test 3, first bending, center span.

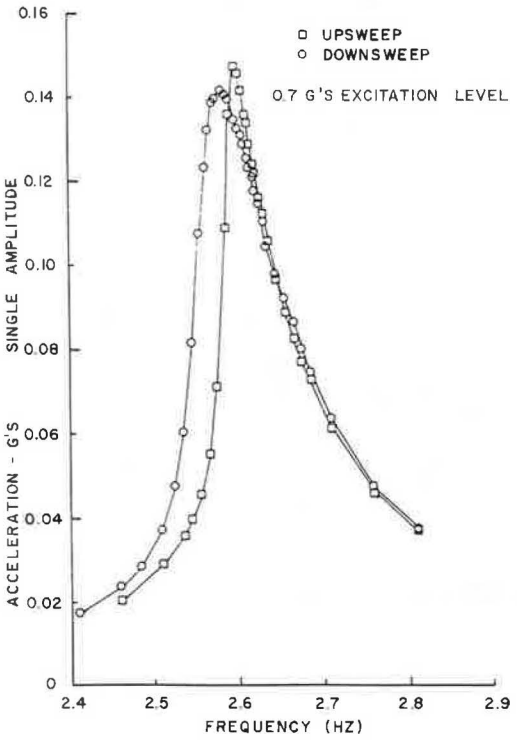

Table 2. Damping ratios determined from half-power-bandwidth method.

Test No.	Damping Ratio (% critical) by Span		
	East	Center	West
First Bending			
1	1.59	1.54	1.60
2	1.22	1.18	1.23
3	1.44	1.38	1.43
4	2.02	1.96	2.02
First Torsion			
1	2.00	1.82	1.98
2	2.06	1.82	1.95
3	1.40	1.39	1.36
4	2.30	1.88	2.17
Second Bending			
1	1.44	1.86	1.32
2	1.56	2.35	1.37
3	1.53	2.66	1.36
4	1.31	2.42	--

Acoustic-Emission Test

When a structure is under load, elastic stress waves called acoustic emissions are generated by plastic deformations that occur at imperfections in the material. These emissions can be detected by a

Figure 5. Driving-point impedance, tests 3 and 4, west span.

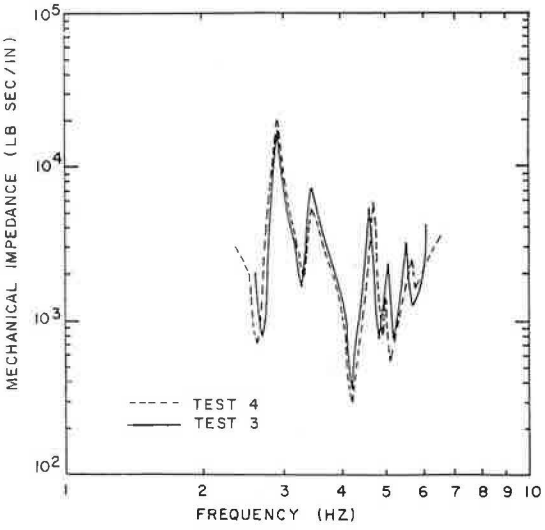

Figure 6. Transfer impedance, tests 3 and 4, center span.

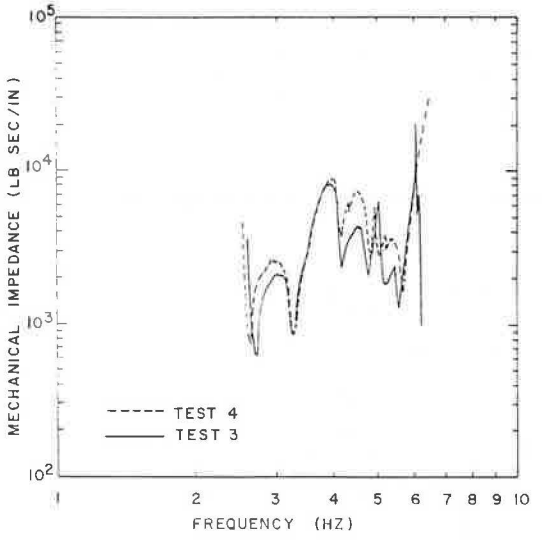

piezoelectric sensor. In the bridge tests, the analog signal from the sensors was converted to an amplitude count analogous to the amplitude of the oscillations in the sensor. Essentially, the sensor converted low-level stress waves to transient electrical signals that corresponded to resonant oscillations of the piezoelectrical element. The amplitude count was based on a time interval the duration of which was proportional to the peak amplitude of the oscillations of the piezoelectric sensor element.

The XY-graphs of amplitude versus time for intervals of 150 s on an intermittent basis did not display the data in a form convenient for evaluating probable crack growth in the welds and base metal where the cover plates terminated. Hence, the amplitude counts were digitized, and a mean value and a standard deviation were calculated for each 150-s interval.

Mean values of the amplitude count per second for each of the 14 data sets for sensors 2 and 6 are shown in Figure 9. These sensors were located on the south interior girder approximately 60 ft from

Figure 7. Spectra of first bending mode response, center span, tests 3 and 4.

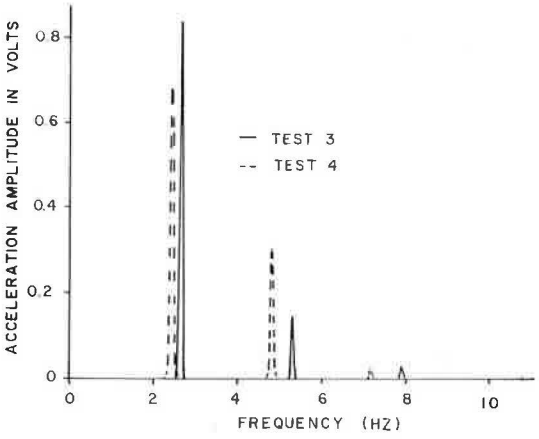

the location of the impending fracture at midspan. Figure 10 illustrates the amplitude count for sensors 1 and 8. Sensor 8 was located on the north exterior girder in the east span and sensor 1 was located on the south exterior girder in the west span. The amplitude count for all sensors was at its maximum at 370 000 fatigue cycles. This notable high count was attributed to the fracture that was probably occurring when the acoustic-emission data were recorded. Visual observation established that the fracture had completely severed the bottom flange and web of the girder approximately 25 min after these data were obtained.

Failures also occurred in the girder flanges within 3 ft of sensors 1 and 6. Ultrasonic inspections revealed these failures after 462 000 and 453 000 fatigue cycles, respectively. The maximum nominal tensile stress due to dead load, ballast, and inertial load at these locations was 103 MPa (15 ksi). However, the growth of fatigue cracks at these locations was not discernible in the recorded emission count.

SUMMARY AND CONCLUDING REMARKS

The intent of this study was to evaluate several vibration-response methods for monitoring structural deterioration. These methods were applied during a fatigue test to determine prescribed dynamic properties of a full-scale bridge.

The damping ratios range between 1 and 3 percent. There were indications that the damping increased and subsequently decreased. The increase may have been caused by mechanical abrasion between adjacent surfaces in the cracks in the concrete deck. Once the cracks became large, the abrasive action ceased and this form of energy dissipation was eliminated. The slipping of the guardrail connections and the friction in the girder support hinges and rocker bearings also contributed to the overall damping. During the fatigue test the variation in damping ratios was not significant from the viewpoint of structural monitoring.

Mechanical impedance is a direct approach to establish typical vibration signatures for a structure. However, there may be a drawback to using impedance as a vibration signature. Impedance (force/velocity) has the characteristics of damping, and damping is the least-known property of a structure.

Stiffness changes, in principle, are directly related to structural deterioration. Resonant frequencies are also a measure of deterioration because

Figure 8. Change in diagonal coefficients of stiffness matrix.

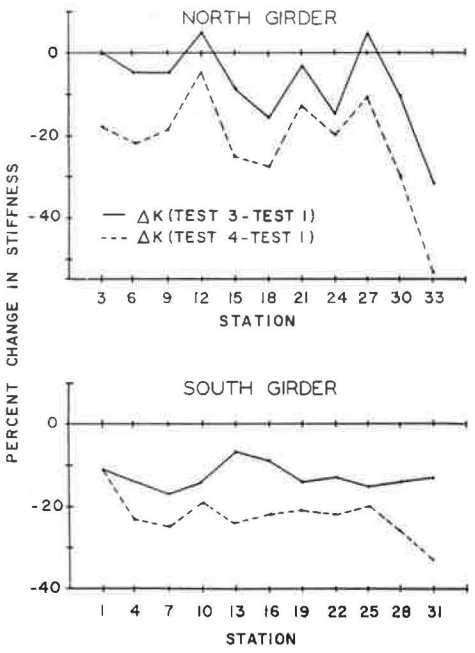

Figure 9. Acoustic emission amplitude count during fatigue test, sensors 2 and 6.

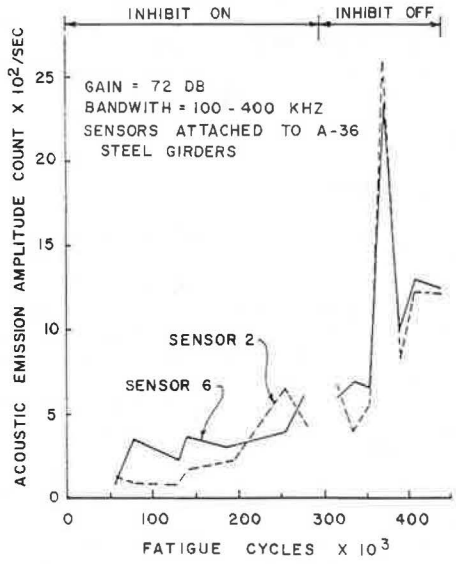

they are proportional to the square root of stiffness. On the basis of an arbitrary analytical model, a change of 20-40 percent in selected stiffness coefficients was observed. However, there was no apparent clue to the location of the fracture in the south interior girder from the changes in the stiffness coefficients for the 22-df model with its restricted coupling. To better simulate the physical behavior of the bridge by coupling all 22 df would require that 12 experimental modes be determined.

Changes in mode shapes were also indications of structural deterioration. When mode shapes are used for this purpose, the vibrational modes should be selected to provide significant response of the particular members that are being monitored. This

Figure 10. Acoustic emission amplitude count during fatigue test, sensors 1 and 8.

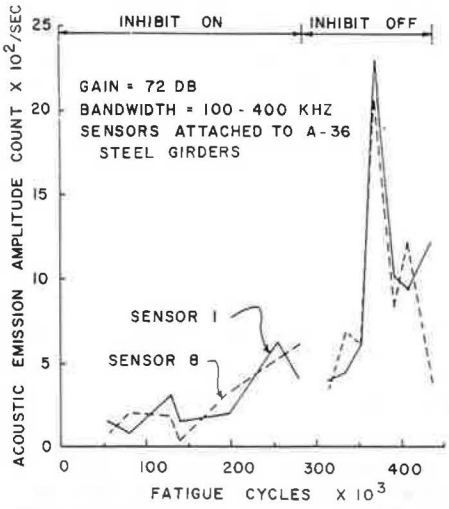

was evident when only the first-bending-mode shape in the bridge showed a marked change after the fracture in the girder.

The relatively slow growth of fatigue cracks in the critical fatigue regions under cyclic loading was not discernible with the acoustic-emission setup used in the bridge test. Extraneous noise from the hydraulic actuator and movement of the bridge on its supports tended to interfere with the acoustic-emission signals. Concrete undergoing permanent deformation also has emission signals that are higher than those from most metals.

All eight sensors were able to detect the critical crack growth in the south interior girder. The use of acoustic-emission sensors shows considerable promise for monitoring structural deterioration under dynamic service loads.

ACKNOWLEDGMENT

We are pleased to acknowledge with gratitude the following individuals and organizations for their contributions to this study: Missouri State Highway Department for sponsoring the project; U.S. Army Corps of Engineers for providing the test bridge; Federal Highway Administration for the use of a data acquisition system and providing the services of Harry Latz, engineering technician; and Robert K. Brady and Ivan E. Lindner, former graduate students, for evaluating the data and reporting the results in their M.S. theses.

REFERENCES

1. R.D. Begg and A.C. McKenzie. Monitoring of Offshore Structures Using Vibration Analysis. Proc., Illuminating Engineering Society Symposium on Integrity of Offshore Structures, Glasgow, Scotland, April 1978.
2. J.K. Vandiver. Detection of Structural Failure on Fixed Platforms by Measurement of Dynamic Response. Proc., Offshore Technology Conference, Vol. 2, OTC 2267, May 1975, pp. 243-252.
3. M.E. Wojnarowski, S.G. Stiansen, and N.E. Reddy. Structural Integrity Evaluation of a Fixed Platform Using Vibration Criteria. Proc., Offshore Technology Conference, Vol. 3, OTC 2909, May 1977, pp. 247-256.

4. R.N. Coppolino and S. Rubin. Detectability of Structural Failures in Offshore Platforms by Ambient Vibration Monitoring. Proc., Offshore Technology Conference, Vol. 4, OTC 3865, May 1980, pp. 101-110.
5. I.E. Lindner. Dynamic Behavior of a Composite Highway Bridge. Univ. of Missouri-Columbia, Columbia, M.S. thesis, 1976.
6. R.K. Brady. An Experimental Study of the Dynamic Characteristics of a Composite Highway Bridge. Univ. of Missouri-Columbia, Columbia, M.S. thesis, Aug. 1977.

Publication of this paper sponsored by Committee on Dynamics and Field Testing of Bridges.

Fatigue Cracks and Their Detection

J.W. BALDWIN, JR., H.J. SALANE, AND R.C. DUFFIELD

A three-span continuous composite bridge of modern design was field tested under fatigue loading that produced stresses equal to or greater than design stresses. During the fatigue loading, a regular inspection schedule was carried out by using radiographic, ultrasonic, and visual methods. Ultrasonic inspection was the most reliable and, in the regions inspected regularly, no cracks are known to have grown to a length greater than 38 mm (1.5 in) before detection. Radiography was nearly as reliable as ultrasonic inspection where it could be used, but more than half the material to be inspected was inaccessible to radiography. A total of 18 fatigue cracks developed at the ends of welded cover plates and 2 fatigue cracks developed in base metal not adjacent to welds. At 471 000 cycles of loading, these cracks had propagated far enough to completely sever the girder flanges at five different sections. The fatigue life in regions where the stress range was 155 MPa (22.5 ksi) was considerably longer than would be predicted on the basis of current code requirements. However, the fatigue life in regions where the stress range was only 60 MPa (8.7 ksi) was considerably shorter than would be predicted on the basis of current code requirements.

During the past two decades, concern about the potential for fatigue failures in highway bridges has increased dramatically. Major laboratory studies have been carried out to determine load versus fatigue-life relationships and to establish design criteria (1,2). The design code of the American Association of State Highway Officials (AASHO) (3), which made little reference to fatigue considerations in the 1950s, now contains highly restrictive fatigue considerations that virtually eliminate certain types of construction. An intensive inspection program has been instituted by the Federal Highway Administration (FHWA) to evaluate the condition of bridges that were designed and constructed before fatigue was recognized as a serious problem.

Laboratory studies are by far the most efficient and cost-effective means of determining fundamental behavior modes in structures, but a certain amount of extrapolation is always required when design criteria for full-scale structures are developed from laboratory data. This is particularly true in the case of fatigue because fatigue behavior is highly sensitive to fabrication details, which are extremely difficult to model in scaled-down laboratory studies. Thus, an occasional check of design criteria through testing of full-scale structures under controlled loading conditions is highly desirable. An unusual opportunity to conduct such a test was created when flood-control work by the U.S. Army Corps of Engineers on the St. Francis River in southeast Missouri necessitated the removal of a 12-year-old highway bridge.

OBJECTIVES

The entire bridge was to be loaded cyclically at stress levels equal to or greater than service-load stresses until one or more girders failed. Objectives of the test were twofold. First, the fatigue behavior of the bridge was to be observed and compared with both laboratory results and current design criteria.

Before loading began and periodically during the test, the bridge was to be inspected by using several modern crack-detection techniques. The second objective, then, was to compare these techniques and to evaluate the effectiveness of each. This was to be the equivalent of inspecting a bridge every few years for its entire lifetime under normal service conditions. Since small cracks missed during one or more inspections would eventually grow into large cracks or failures, this procedure would provide information concerning sizes and types of cracks that are likely to be missed as well as those that are likely to be found.

DESCRIPTION OF TEST BRIDGE

The two-lane bridge was made up of three [21.9, 28.3, and 21.9 m (72, 93, and 72 ft)] continuous concrete-on-steel composite-girder spans. It was designed during early 1962 according to 1961 AASHO specifications for one H15-44 loaded lane. [For a general schematic of the bridge, see Figure 1 in Salane, Baldwin, and Duffield in this Record; see also the report by Salane and others (4).] Girders and cover plates were of American Society for Testing and Materials (ASTM) A36 steel, and the unshored slab was cast from concrete with a 28-day compressive strength of 36.6 MPa (5720 psi). Shear connectors were C4x5.4 channels 159 mm (6.25 in) long fillet-welded to the top flanges of the girders.

Channel diaphragms 460 mm (18 in) deep bent from 610x8-mm (24x0.31-in) plates were bolted to 114x9.5-mm (4.5x0.38-in) bearing stiffeners over the supports and to 76x9.5-mm (3x0.38-in) web stiffeners in the spans. There were two intermediate diaphragms in each end span and four intermediate diaphragms in the center span.

DESCRIPTION OF FATIGUE TEST

A total of 471 000 fatigue cycles were applied to the bridge over a period of approximately five weeks. Desired dynamic stress ranges were obtained by exciting the bridge at its first-bending-mode resonant frequency by using the closed-loop electrohydraulic shaker shown in Figure 1. This shaker consisted of 40 kN (9 kips) of steel weights attached to the top of an 89-kN (20-kip) servocon-